

9. SITE 1158¹

Shipboard Scientific Party²

PRINCIPAL RESULTS

Site 1158 is located in Zone A, 78 km south of Site 1157. The site is located in a sediment-filled, axis-parallel basin near the eastern margin of the depth anomaly, ~60 km east of the ~127°E fracture zone. The sea-floor magnetic age is ~20 Ma. This site is one of six (together with Sites 1153, 1157, 1161, 1162, and 1159) along a generally north-south line that were intended to locate possible occurrences of Indian-type mantle beneath western Zone A.

Hole 1158A was spudded in ~5167 m water depth and was washed through 199 m of sediment, of which only 1.9 m of drilling-disturbed material was recovered. Rotary drilling penetrated 14.4 m into basement, recovering 0.8 m (5.9%) of aphyric to sparsely olivine-plagioclase phyric basalt with a few glassy rinds. Veins and vesicles in the basalt are filled with silica and clay, in contrast to the carbonate-dominated vein material seen in cores from previous sites. Hole 1158A was abandoned because of poor drilling conditions.

At Hole 1158B, 270 m north of Hole 1158A, we washed through 126 m of sediment, recovering 1.6 m of disturbed brown clay with rare thin intervals containing coarse angular basalt fragments. We continued drilling 15 m into basement, recovering 1.6 m (10.7%) of aphyric to sparsely olivine-plagioclase phyric basalt with visible groundmass clinopyroxene. The basalt is slightly to moderately altered with olivine phenocrysts and a microcrystalline groundmass being partially replaced by Fe oxyhydroxides and smectite. Hole 1158B was also abandoned because of drilling problems.

At Hole 1158C, 170 m farther north, we washed through 108 m of sediment with no recovery and drilled 9.4 m into basement, recovering 1.61 m (17.1%) of massive diabase beneath overlying aphyric basalt rubble. The diabase is composed of plagioclase, clinopyroxene, and magnetite/ilmenite with a medium-grained subophitic texture. Low-

¹Examples of how to reference the whole or part of this volume.

²Shipboard Scientific Party addresses.

temperature alteration products (primarily Fe oxyhydroxide and clay) are present throughout the core.

Two glass samples from Holes 1158A and 1158B are quite primitive, with MgO contents of 9.1 and 8.2 wt%, respectively. As in all Leg 187 sites, the associated whole rocks have lower MgO contents than the glasses, ranging from ~8.2 wt% for Hole 1158A to 6.6 and 6.2 wt% in the Hole 1158B basalt and the Hole 1158C diabase. These lower values seem more likely attributable to alteration than to crystallization effects. Relative to 0- to 7-Ma Zone A basalts, Site 1158 glasses have low CaO/Al₂O₃ ratios and high Na₂O, TiO₂, Zr, and Y contents, similar to lavas of the Segments A2 and A3 propagating rift tips. Ba and Zr systematics indicate that Site 1158 lavas were derived from Pacific-type mantle <2 m.y. after the Indian-type lavas of Site 1157 were erupted on the same flow line. This rapid change in mantle source is comparable in temporal and spatial scale to the 0- to 4-Ma migration documented by dredging in Segment B5 to the south.

OPERATIONS

Transit to Site 1158

Because of high winds and heavy seas the 42-nmi transit from Site 1157 to Site 1158 took nearly 7 hr, and we could not deploy the geophysical gear. We dropped a positioning beacon on the prospectus Global Positioning System coordinates at 1715 hr on 15 December. Water depth as measured by the precision depth recorder at this site is 5178.4 m. The nine-collar bottom-hole assembly employed on the earlier sites was made up with a new C-7 four-cone rotary bit.

Hole 1158A

We began operations by washing down through the sediment column until we contacted basement at 198.9 meters below seafloor (mbsf). The wash barrel was retrieved, and we deepened the hole by rotary coring to 213.3 mbsf. We deployed fluorescent microspheres as a tracer for microbiological infiltration analysis on Core 187-1158A-2R. Rapid penetration, high and erratic torque during drilling, and poor recovery (~6%; see Table T1) in the two core barrels we retrieved led to our abandoning this hole. The drill string cleared the seafloor at 1330 hr on 16 December, and we offset 200 m north, where our precruise site survey indicated thinner sediment cover.

Hole 1158B

After washing through the sediment column to 126.2 mbsf and recovering the wash barrel, we rotary cored in basement to 141.2 mbsf before unstable hole conditions forced us to abandon Hole 1158B. Microbiological tracers (microspheres) were deployed on Core 187-1158B-3R. The bit cleared the seafloor at 0545 hr on 17 December; we offset another 200 m north to attempt a third hole at this site.

Hole 1158C

We contacted basement at 108.0 mbsf in Hole 1158C and recovered the wash barrel and a single rotary core barrel (108.0–117.4 mbsf, 17%

T1. Coring summary, Site 1158, p. 24.

recovery) before poor hole conditions again precluded continuing operations. Microsphere tracers were deployed on Core 187-1158C-2R. Based on our experience thus far and on the recovery of sufficient material to meet our primary objectives, we chose to end operations at this site. The drill bit cleared the seafloor at 1420 hr and the rotary table at 2315 hr on 17 December.

IGNEOUS PETROLOGY

Introduction

Holes 1158A, 1158B, and 1158C were cored into basement at this site. Hole 1158A penetrated 14.4 m into basement, recovering 0.85 m of basalt core from three sections (Sections 187-1158A-1W-2, 2R-1, and 3R-1), a net recovery of 5.90%. Hole 1158B penetrated 15.0 m into basement, recovering 1.6 m of core from three sections (Sections 187-1158B-2R-1, 3R-1, and 4R-1), a net recovery of 10.67%. Hole 1158C penetrated 9.4 m into basement, recovering 1.61 m of core from three sections (Sections 187-1158C-1W-1, 2R-1, and 2R-2), a net recovery of 17.13%.

Hole 1158A

All basalt recovered from this hole is included in one lithologic unit: aphyric to sparsely olivine-plagioclase phyric basalt. Glassy rinds, chilled margins, and the wedge-shaped, fracture-controlled morphology of some pieces (e.g., Section 187-1158A-1W-2 [Piece 1]) indicate that these are fragments of pillow lava. Pieces range from ~1 cm to several centimeters in size (i.e., less than the core diameter) and are therefore unoriented. The color of the basalt varies from gray to brownish gray, reflecting local differences in degree of alteration that range from slight to moderate (see “[Hole 1158A](#),” p. 5, in “Alteration”).

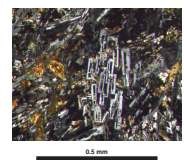
Olivine phenocrysts are generally equant and euhedral to subhedral; plagioclase phenocrysts are tabular to prismatic. Approximately 20% of the phenocrysts are present as single-phase or two-phase glomerocrysts. Four of the five pieces in Section 187-1158A-1W-2 have between 1.5% and 2.5% total phenocryst content, with olivine and plagioclase in roughly equal amounts (the average size of both phases is ~0.8 mm). One of the nine pieces in Section 187-1158A-2R-1 has a similar phenocryst population. The remaining pieces in both sections are aphyric. Section 187-1158A-3R-1 contains ~1% olivine and ~0.5% plagioclase microphenocrysts (~1 mm).

In most cases, the groundmass is fine grained. Section 187-1158A-2R-1 (Piece 3) is unusual in that it is aphyric but has a grainy texture and a coarser groundmass (fine to medium grained; 0.5–1 mm) than the other aphyric pieces in this section. Partial replacement of glassy groundmass by brown clays highlights the spherulitic texture of chilled margins in Section 187-1158A-2R-1. In addition to spherulites, the chilled margins are composed of plagioclase crystals with parallel “box” structures (Figs. [F1](#), [F2](#)), indicating rapid cooling. The edges of some subhedral to anhedral prismatic plagioclase phenocrysts in these chilled margins also have overgrowths of box-textured plagioclase that are in optical continuity with the phenocryst (e.g., Sample 187-1158A-2R-1 [Piece 1]; Fig. [F3](#)).

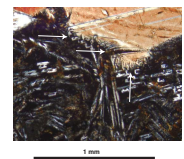
F1. Parallel-growth box-textured plagioclase in basalt, p. 12.



F2. Parallel-growth box-textured plagioclase, p. 13



F3. Plagioclase box overgrowths on a plagioclase phenocryst, p. 14.



Away from the chilled margins, groundmass plagioclase is locally flow aligned on a thin-section scale. In addition, where olivine (or olivine and plagioclase) glomerocrysts are present, some groundmass plagioclase forms snowball textures around the glomerocrysts (e.g., Section 187-1158A-3R-1 [Piece 3]; Fig. F4). In Piece 3, olivine is seriate, ranging from ~1 mm microphenocrysts to groundmass crystals <10 µm in size. Olivine is generally equant and euhedral. About 60% of the microphenocrysts are replaced by Fe oxyhydroxide throughout this core, but it is fresh outside oxidized zones in Section 187-1158A-3R-1. Mn oxide, either as spots or as a continuous coating, is present on weathered (oxidized) uncut surfaces.

Hole 1158B

All basalts from this hole are included in one lithologic unit: aphyric to sparsely olivine-plagioclase aphyric basalt; phenocryst variations are similar to those from Hole 1158A, Unit 1. Color depends on the groundmass grain size and the degree of alteration. Pieces with microcrystalline to very fine grained groundmass range from medium to dark gray where fresh and to whitish gray where altered. Those with a fine-grained groundmass are medium gray where fresh and brownish gray where altered. As in Hole 1158A, most pieces are <3 cm in size and therefore unoriented relative to the core. They have weathered, uncut surfaces with alteration halos. Overall, alteration ranges from slight to moderate (see “[Hole 1158B](#),” p. 6, in “Alteration”).

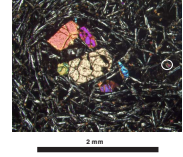
Phenocryst abundance ranges between 0% and 2%, of which olivine comprises ~55% and plagioclase ~45%; both phases are <2 mm in size. Plagioclase phenocrysts are mainly tabular to prismatic and euhedral, although 1- to 2-mm rounded to subrounded plagioclase occurs in some places in Section 187-1158B-4R-1. Glomerocrysts of olivine and plagioclase make up as much as 40% of the phenocryst content in some pieces (e.g., Section 187-1158B-3R-1 [Piece 2]). Many of the plagioclase phenocrysts (~50%) throughout this hole have a wide range of disequilibrium textures, including concentric oscillatory zoning (e.g., Section 187-1158B-2R-1 [Piece 1]; Fig. F5), discontinuous twin planes, and sieve textures.

Groundmass is generally fine grained (<1 mm) but approaches medium grained (~0.9 mm) in some pieces (e.g., Section 187-1158B-2R-1 [Pieces 10 to 14]); the latter have a grainy texture like Section 187-1158A-2R-1 (Piece 3). In Section 187-1158B-2R-1, 10 of the 14 pieces have a similar grainy texture. In many of these pieces, groundmass plagioclase (~0.9 mm) forms a felty texture with clinopyroxene filling the interstices (e.g., Piece 1). Clinopyroxene in the groundmass varies from discrete euhedral to anhedral crystals (e.g., 187-1158B-2R-1 [Piece 1]; Fig. F5) and subophitically encloses plagioclase in the grainy textured pieces (e.g., Section 2R-1 [Piece 13]). Clinopyroxene in the groundmass ranges from ~0.5 to 1.5 mm in size, although varying degrees of strain extinction and areas of small anhedral crystals in which new subgrain boundaries have formed sometimes obscure original grain boundaries. Five pieces in Section 187-1158B-4R-1 have altered glassy rinds.

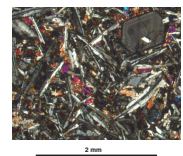
Hole 1158C

There are two lithologic units in Hole 1158C. This hole also has the highest percentage (~25%) of oriented pieces at this site.

F4. Snowball plagioclase around an olivine glomerocryst, p. 15.



F5. Plagioclase with concentric oscillatory zoning in a groundmass of plagioclase and clinopyroxene, p. 16.



Unit 1

Unit 1 (Section 187-1158C-1W-1 to Section 2R-1 [Piece 8]) consists of aphyric to sparsely olivine-plagioclase phyric basalt rubble with a range in grain size and textures similar to that seen in Holes 1158A and 1158B (see “[Hole 1158A](#),” p. 3, and “[Hole 1158B](#),” p. 4).

Unit 2

Unit 2 (Section 187-1158C-2R-1 [Piece 8] to Section 2R-2) is a diabase, defined by its subophitic texture and medium grain size (1–5 mm). Thin section shows this to consist of plagioclase and clinopyroxene in roughly equal proportions with ~2% equant to skeletal opaque minerals. The color of this unit is light brownish gray; the brown coloration is due to alteration and Fe staining of plagioclase; overall, alteration ranges from moderate to high (see “[Hole 1158C](#),” p. 6, in “Alteration”). The subophitic texture (Fig. F6) is visible in hand specimen (e.g., Section 187-1158C-2R-1 [Piece 13]). Grain size decreases with depth through Section 187-1158C-2R-2, but a grainy texture persists in hand specimen. Section 187-1158C-2R-2 is also more vesicular (5%–7%) than either the diabase in shallower sections in this hole or the basalts from this and earlier sites. The vesicles are spherical, average 0.7 mm in diameter, and are filled by a cream-tan clay/silicate mixture.

The systematic decrease in groundmass grain size, beginning 30 cm from the bottom of Section 187-1158C-2R-1 and extending through Section 2R-2, may be interpreted as a finer grained marginal facies of Unit 2. There is no evidence indicating whether Unit 2 is a flow or an intrusion.

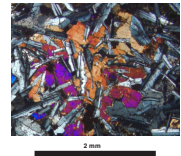
ALTERATION

Hole 1158A

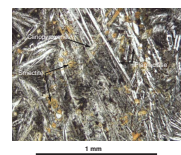
Basalt from Hole 1158A is slightly to moderately altered. Most of the basalt pieces are subangular and 2–5 cm in diameter, and these have weathered, uncut surfaces, indicating that this is rubble. Uncut surfaces of all pieces have spots or coatings of Mn oxide (as thick as 1 mm in Sample 187-1158A-1W-2 [Piece 5]) and/or thin (<0.2 mm) patches of white cryptocrystalline silica, which is commonly associated with spots of Mn oxide. Alteration halos extend 6–8 mm from the edges into the pieces. Within these halos, olivine is mostly (70%) replaced by Fe oxyhydroxides, and groundmass is replaced by smectite. The intensity of alteration does not change systematically downhole. Vesicles (1%; ~0.5 mm) are lined with bluish cryptocrystalline silica or yellowish green smectite. The vein density averages 1.1/m of core. Rare veins are ~1 mm wide and filled with silica that is in places Fe stained. The veins are surrounded by up to 2-mm-wide oxidation halos in which the groundmass is replaced by Fe oxyhydroxide and smectite. Within the fresher parts of the basalt, groundmass olivine ranges from fresh (e.g., Section 187-1558-3R-1) to 60% replaced by Fe oxyhydroxide. Replacement of groundmass by smectite is also common (Fig. F7).

The outermost layer of some glassy margins (e.g., Section 187-1158A-1W-2 [Piece 1]) consists of brownish orange, up to 2-mm-thick, dense palagonite that gives the altered glass a cherty appearance not seen in the previous sites. Bleached and partly silicified spherulitic quench

F6. Subophitic texture, p. 17.



F7. Smectite replacement of groundmass in basalt, p. 18.



zones are also common. In places, Fe oxyhydroxide and clay partially replace the glassy groundmass of the spherulitic quench zone and thereby highlight spherulite textures (spherulitic vs. coalesced spherulites).

Hole 1158B

Basalt in Sections 187-1158B-2R-1 and 3R-1 shows only slight low-temperature alteration effects, whereas Section 187-1158B-4R-1 is moderately altered. Uncut surfaces are generally weathered to a buff color, with oxidation halos reaching 0.5–10 mm into the basalt, suggesting again that this is rubble. Surficial coatings such as Mn oxide spots, silica, or sediment are absent. Vesicles (<1%, 0.5 mm) are variably filled or lined with Mn oxide, smectite, or bluish cryptocrystalline silica. The average vein density is 0.6/m, but the combined fracture + vein density averages 21.2/m, which is higher than in Hole 1158A (8.9/m). The rare veins are <1 mm wide, filled with silica (in places Fe stained), and usually surrounded by 1- to 8-mm-wide oxidation halos. Fractures are lined with Mn oxide or cryptocrystalline silica. Minute fractures commonly extend from phenocrysts into the groundmass or appear to migrate around phenocrysts. Both observations may reflect the rheological differences between phenocrysts and groundmass.

Olivine phenocrysts are most severely altered (100%) within the oxidation halos of the weathered margins and are partially (65%–80%) replaced by Fe oxyhydroxides and smectite in the fresher interiors. Plagioclase phenocrysts are fresh throughout, except within oxidation halos, where ~3% are replaced by a cream-white clay. Within the slightly altered sections <10% of the groundmass is replaced by Fe oxyhydroxide and smectite, whereas moderately altered sections display 10%–20% alteration of the groundmass to Fe oxyhydroxide and smectite. Glass rinds were only recovered in Section 187-1158B-4R-1 and, generally, are partially altered to palagonite that is dissected by quartz filled veins (<0.3 mm), the majority of which are aligned subparallel to the chilled margin. In places, palagonite is coated with bluish silica. The groundmass of chilled margins (spherulitic through coalesced spherulite zones) is partly replaced by a white-gray mixture of clay/silica and rarely by brown Fe oxyhydroxide, which highlights spherulites up to 1.5 mm in diameter.

Hole 1158C

Aphyric basalt of igneous Unit 1 (see [“Igneous Petrology,”](#) p. 3) is slightly to moderately altered with <10%–20% of groundmass replaced by Fe oxyhydroxides and smectite. Again, buff weathered surfaces on the uncut surfaces of pieces in Section 187-1158C-1W-1 suggest that this is rubble. As noted for Hole 1158B, surface coatings such as Mn oxide spots, silica, or sediment are not present. Vesicles (<1%) are filled with smectite and/or Fe oxyhydroxide. Rare open fractures are <1 mm wide; some are lined with smectite, and a few are surrounded by up to 2-mm-wide oxidation halos. Groundmass olivine is mostly (~60%) replaced by Fe oxyhydroxide; replacement of groundmass by smectite and Fe oxyhydroxide ranges from ~10% to 20% overall.

Diabase of igneous Unit 2 (see [“Igneous Petrology,”](#) p. 3) appears moderately to highly altered in hand specimen because of pervasive Fe staining and the subophitic texture that gives the rock a friable texture and grainy appearance. The uncut surfaces are weathered brown but are

free of Mn oxide, silica, or sediment coatings. In some cases (e.g., Section 187-1158C-2R-1 [Pieces 9 and 14]), oxidation halos extend as far as 15 mm from weathered fracture surfaces into the diabase and are marked by higher abundances of Fe oxyhydroxide. Throughout the section, veins are absent, and the fracture density is comparatively low, with 3.4 fractures per meter of core. Vesicles (5%–7%; ~1 mm) are filled with yellowish smectite, Fe-stained silica, and, rarely, Mn oxide. In Pieces 19–27 of Section 187-1158C-2R-1, 10% of plagioclase is replaced by a pale clay. Inspection under the binocular microscope or in thin section reveals that alteration of groundmass clinopyroxene to Fe oxyhydroxide/smectite has caused pervasive Fe staining of plagioclase (Fig. F8), giving the rock a more altered appearance than its actual slightly to moderately altered status.

MICROBIOLOGY

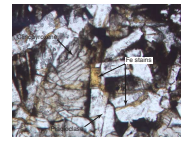
At Site 1158 two rock samples (Samples 187-1158A-2R-1 [Piece 8, 34–37 cm] and 187-1158C-2R-1 [Piece 10, 54–57 cm]) were collected to characterize the microbial community inhabiting this environment (Table T2). Both samples were pillow basalt fragments composed of crystalline basalt only (see “Igneous Petrology,” p. 3). To sterilize them, the outer surfaces of the rock samples were quickly flamed with an acetylene torch, and enrichment cultures and samples for high-pressure enrichment, DNA analysis, and electron microscope studies were prepared (see “Igneous Rocks,” p. 7, in “Microbiology” in the “Explanatory Notes” chapter).

To evaluate the extent and type of contamination caused by drilling fluid, fluorescent microsphere tests were carried out for both rock cores. Surface seawater was collected for DNA characterization (Table T2; also see “Tracer Test,” p. 9, and “Surface Seawater,” p. 8, in “Microbiology,” in the “Explanatory Notes” chapter). Pieces from each core were rinsed in nanopure water, the collected water was filtered, and the filters were examined for the presence of microspheres under a fluorescence microscope. Thin sections were used to examine the extent of contamination inside the samples. Microspheres were detected on the filters; in the thin sections microspheres were found both inside fractures and on the thin-section surface. All were located close to the thin-section margins, with the exception of one microsphere that was observed in a large fracture in the thin-section center (Section 187-1158A-2R-1). Five microspheres were observed in thin sections from Core 187-1158A-2R and 13 from Core 187-1158C-2R. Of these, 12 were in a single crack.

SITE GEOPHYSICS

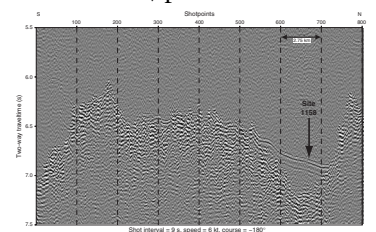
Site selection for Site 1158 was based on a single-channel seismic survey conducted during the *R/V Melville* cruise Sojourner 5 in 1997 (Fig. F9). The prospectus site is near shotpoint 680 of the south-north seismic profile, toward the northern side of a significant basin structure. This seismic profile shows clear sediment cover at Site 1158 from 6.85- to 7.08-s two-way traveltime, giving an estimated sediment thickness of ~230 m. Hole 1158A was drilled through 199 m of sediment before basement was reached, whereas Holes 1158B and 1158C, ~273 and 444 m north of Hole 1158A, encountered only 126 and 108 m of sediment, respectively.

F8. Fe staining of plagioclase along cracks and cleavage planes, p. 19.



T2. Rock samples for cultures, DNA analysis, SEM/TEM, and contamination studies, p. 25.

F9. Seismic profile from *Melville* cruise Sojourner 5 crossing the Site 1158 location, p. 20.



SEDIMENTS

Two wash barrels were recovered from Site 1158. Cores 187-1158A-1W and 187-1158B-1W both contain severely drilling disturbed siliceous sediment and represent drilled intervals of 198.9 and 126.2 m, respectively. Most of the sediment occurs as fragmented drilling biscuits or drilling-induced pellets of densely packed clay of varying color. Overall, medium brown clay is most abundant, with less abundant dark brown and rare brownish gray clay. Both cores contain lithified, siliceous fragments, several centimeters in the longest dimension, that appear to be burrow casts; tabular fragments of the same material also occur in Core 187-1158B-1W. Several intervals (1–2 cm thick) of disseminated, very coarse sand-sized angular basalt chips are also present in Core 187-1158B-1W. The only carbonate identified, which effervesces slightly with dilute HCl (~5%–10%), was from the base of Core 187-1158B-1W.

GEOCHEMISTRY

Introduction

Site 1158 basalts were recovered from three holes (1158A, 1158B, and 1158C) ~78 km south of Site 1157. The site is located on ~20-Ma crust within Zone A at the eastern margin of the depth anomaly. One whole rock from each hole was analyzed for major and trace elements by X-ray fluorescence (XRF) and ICP-AES (inductively coupled plasma-atomic emission spectrometry). Basalt glasses from Holes 1158A and 1158B were analyzed by ICP-AES only (Table T3). Whole-rock Ni and Cr contents determined by ICP-AES are consistently low, and MgO, Fe₂O₃, and Al₂O₃ are consistently high when compared with XRF data.

Hole 1158A

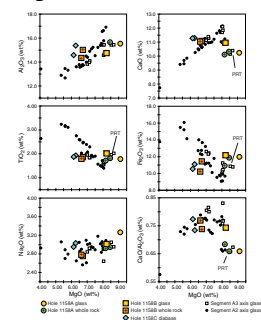
Samples from Hole 1158A are assigned to one lithologic unit, an aphyric to sparsely olivine-plagioclase phyric pillow basalt (see “[Igneous Petrology](#),” p. 3). The Hole 1158A glass is primitive (i.e., ~9.1 wt% MgO) with relatively high Na₂O, Fe₂O₃, Zr, and Y contents and low CaO and CaO/Al₂O₃ values (Figs. F10, F11). The corresponding whole rock has ~0.5 wt% less MgO than the glass, as observed throughout Leg 187 probably as a consequence of alteration (see “[Geochemistry](#),” p. 8). However, based on similarities in most major elements, Hole 1158A whole rock and glass are probably genetically related. The whole rock is lower in Na₂O, slightly lower in Y, and slightly higher in Cr than the associated glass. Alteration of olivine and the consequent loss of Mg from the whole-rock sample could explain the constancy of Ni with decreasing MgO. Accumulation of plagioclase or olivine phenocrysts cannot explain the relatively low Na₂O, Y, Zr and high Cr contents. These variations could indicate retention of clinopyroxene and/or spinel in groundmass while mesostasis ± olivine is lost to alteration. Note that Sr and Ba are unchanged.

Hole 1158B

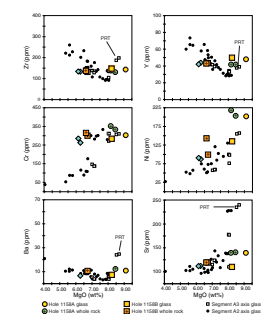
Hole 1158B samples are assigned to a single unit of aphyric to sparsely olivine-plagioclase phyric basalt similar to that of Hole 1158A.

T3. Compositions of basalts from Site 1158, p. 26.

F10. Major element compositions vs. MgO for basalts from Holes 1158A, 1158B, and 1158C compared with Zone A SEIR MORB glasses, p. 21.



F11. Trace element compositions vs. MgO for basalts from Holes 1158A, 1158B, and 1158C compared with Zone A SEIR MORB glasses, p. 22.



Unlike Hole 1158A, the 1158B whole rock is much lower in MgO (~6.7 wt%) than the associated glass (~8.2 wt%). Major and trace element variations are inconsistent with the whole rock being derived from the glass by simple low-pressure crystal fractionation. CaO, Al₂O₃, TiO₂, Zr, and Y are relatively similar in the glass and whole rock, even with a 1.5 wt% decrease in MgO. Furthermore, Na₂O and Fe₂O₃ decrease rather than increase, as would be expected with simple crystal fractionation. Loss on ignition for whole-rock Sample 187-1158B-2R-1, 55–58 cm, is slightly high (1.24 wt%), consistent with MgO loss during alteration.

Hole 1158C

Two lithologic units are recognized in Hole 1158C. Unit 1 is similar to those described in Holes 1158A and 1158B, and Unit 2 is a diabase. Only Unit 2 was analyzed aboard ship. Although lower in MgO, the diabase is similar to Hole 1158B whole-rock Sample 187-1158B-2R-1, 55–58 cm, in many respects. Slightly higher CaO and Al₂O₃ contents could result from plagioclase accumulation, and lower MgO suggests that the diabase has evolved magmatically relative to the Hole 1158B whole rock. However, the scale of variations in MgO introduced by alteration makes petrogenetic interpretations based on whole-rock data highly speculative. The compositional pattern described above (Holes 1158A and 1158B) appears to apply equally to the diabase, suggesting that the unchanging CaO, Al₂O₃, TiO₂, Zr, and Y contents with decreasing MgO may be a complex interplay between in situ crystal growth and alteration effects. Neither of the Site 1158 glass compositions appears to be a simple parent to either the whole rock or the diabase.

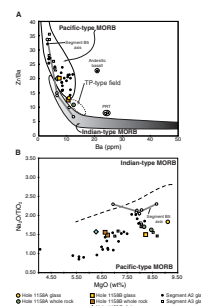
Temporal Variations

Site 1158 basalts are compared to two Zone A propagating rift segments (A2 and A3) in Figures F10 and F11. The Site 1158 glasses exhibit some of the major and trace element characteristics of lavas dredged from propagating rift tips (PRTs) of Segments A2 (127.5°E) and A3 (131.0°E) (Pyle, 1994). In particular, the primitive Hole 1158A glass has low CaO/Al₂O₃ contents, high Na₂O, TiO₂, Zr, and Y, and slightly elevated Sr and Ba, indicating low-degree partial melts. It also has high Fe₂O₃, which suggests a high mean melting pressure (Klein and Langmuir, 1987). These features are less pronounced in the Hole 1158B glass, but its composition overlaps trends defined by PRT glasses from Segments A1 and A2; note the increasing CaO and CaO/Al₂O₃ and decreasing Zr, Y, and TiO₂ with decreasing MgO of Segment A1 and A2 glasses and the general similarity of Site 1158 glasses. The unevolved nature of the Site 1158 glasses (>8.0 wt% MgO) and the variability in major and trace elements indicate that these compositional variations are caused by partial melting with little influence from low-pressure crystal fractionation in subaxial magma systems. This similarity of Site 1158 lavas to lavas recovered in the PRTs of Zone A suggest proximity to a PRT environment for Site 1158 basalts.

Mantle Domain

The Zr/Ba systematics of Site 1158 (Fig. F12A) suggest a Pacific-type mantle. The Hole 1158A glass, Hole 1158B glass, and Hole 1158C diabase have high Zr/Ba and vary within the compositional range of Pa-

F12. Variations of Zr/Ba vs. Ba and Na₂O/TiO₂ vs. MgO for Holes 1158A, 1158B, and 1158C, p. 23.



cific-type mid-ocean-ridge basalt (MORB) from Southeast Indian Ridge (SEIR) Segments A2 and A3 (Fig. **F12B**). The Site 1158A whole rock lies below the main Pacific-type MORB field, toward the PRT field of Segment A3, consistent with low-degree melting (i.e., higher Ba) and with the inference that these lavas are associated with the rift-tip environment. Site 1158 lavas also have $\text{Na}_2\text{O}/\text{TiO}_2$ systematics that suggest a Pacific-type source. Comparing the Site 1158 results with those from Sites 1153 and 1157 (see “**Geochemistry**” p. 6, in the “Site 1153” chapter and “**Geochemistry**,” p. 11, in the “Site 1157” chapter), we identify Pacific-type mantle beneath western Zone A at 28 Ma (Site 1153) and 20 Ma (Site 1158), with intervening Indian-type mantle at 22 Ma (Site 1157). These fluctuations in mantle source are on a time and space scale similar to that of the recent Pacific-type source migration across Segment B5 (Pyle et al., 1992).

REFERENCES

- Klein, E.M., and Langmuir, C.H., 1987. Global correlations of ocean ridge basalt chemistry with axial depth and crustal thickness. *J. Geophys. Res.*, 92:8089–8115.
- Pyle, D.G., 1994. Geochemistry of mid-ocean-ridge basalt within and surrounding the Australian Antarctic Discordance [Ph.D. dissert.]. Oregon State Univ., Corvallis OR.
- Pyle, D.G., Christie, D.M., and Mahoney, J.J., 1992. Resolving an isotopic boundary within the Australian-Antarctic Discordance. *Earth Planet. Sci. Lett.*, 112:161–178.

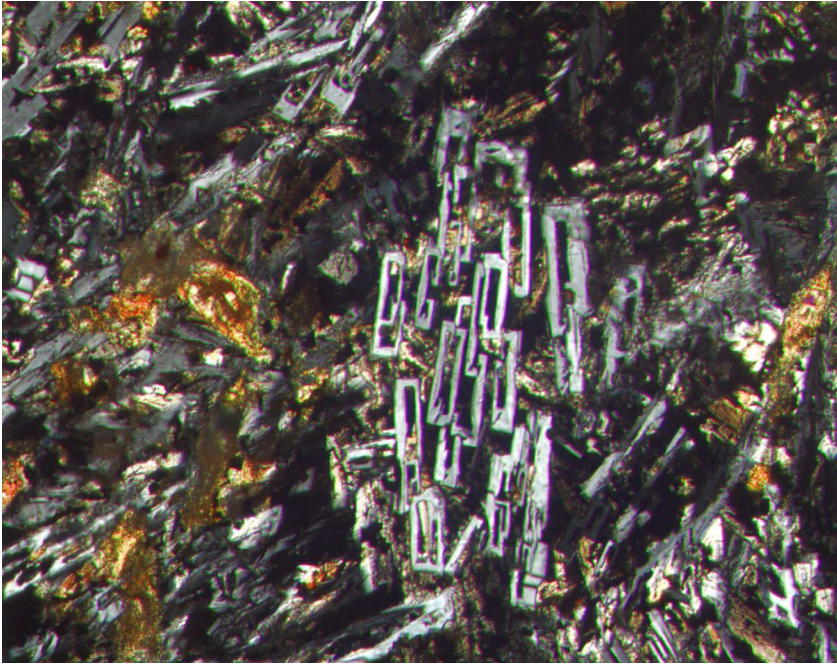
Figure F1. Photomicrograph in plane-polarized light of Sample 187-1158A-2R-1 (Piece 1, 0–4 cm) (see “[Site 1158 Thin Sections](#),” p. 12) showing parallel-growth box-textured plagioclase in a vesicular area of the thin section. See close-up in Figure F2, p. 13.



2 mm



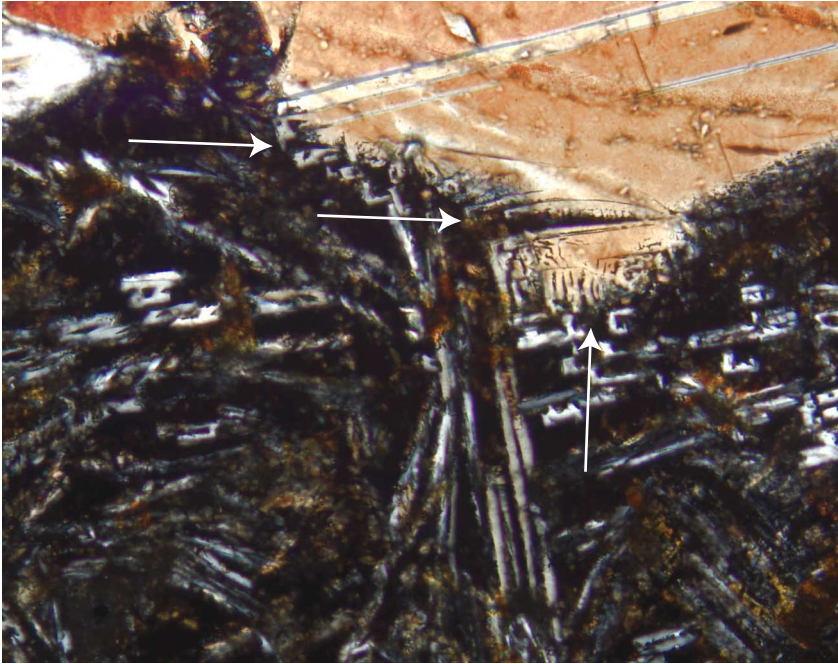
Figure F2. Photomicrograph, with crossed polars, of Sample 187-1158A-2R-1 (Piece 1, 0–4 cm) (see “[Site 1158 Thin Sections](#),” p. 12), showing parallel-growth box-textured plagioclase similar to those seen in Figure F1, p. 12.



0.5 mm



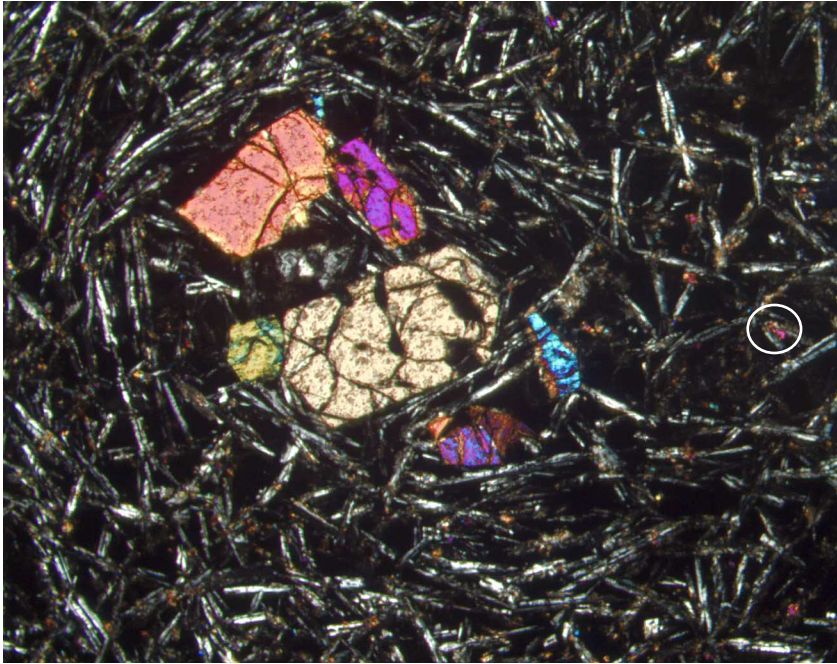
Figure F3. Photomicrograph, with crossed polars, of Sample 187-1158A-2R-1 (Piece 1, 0–4 cm) (see “[Site 1158 Thin Sections](#),” p. 12), showing plagioclase box overgrowths (examples are indicated by arrows) on a plagioclase phenocryst. These overgrowths are in optical continuity with the phenocryst. Note that the thin section is thicker than the standard 30 μm .



1 mm



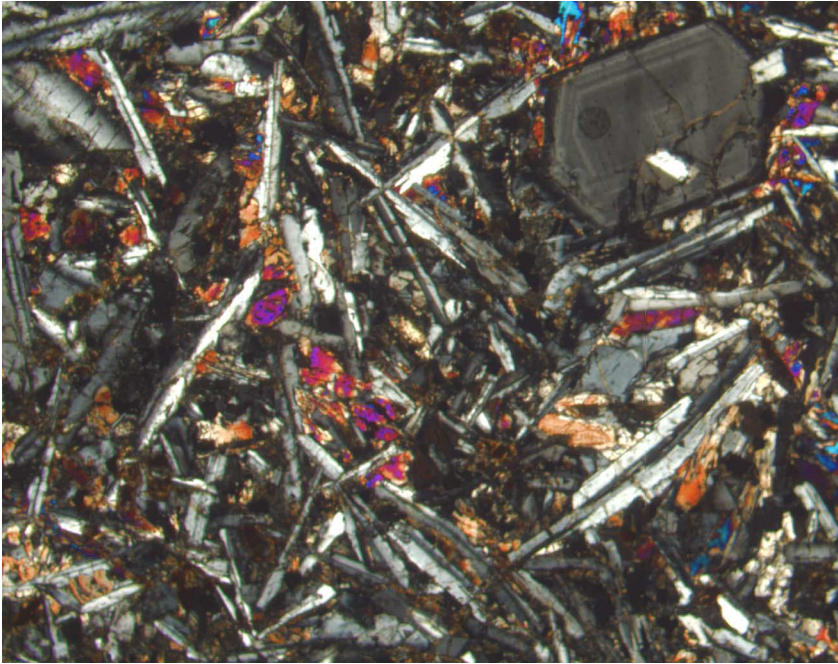
Figure F4. Photomicrograph, with crossed polars, of Sample 187-1158A-3R-1 (Piece 3, 10–13 cm), showing snowball plagioclase around an olivine glomerocryst; apparent rotation is clockwise. All the crystals with second-order birefringence colors in the groundmass are equant olivines (example is circled; see “Site 1158 Thin Sections,” p. 13). Olivine is seriate.



2 mm



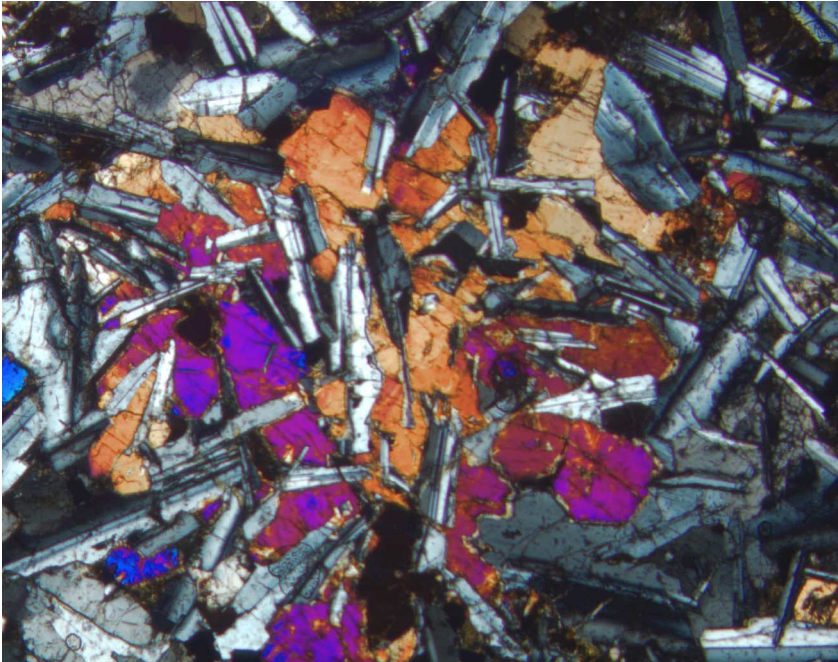
Figure F5. Photomicrograph, with crossed polars, of Sample 187-1158B-2R-1 (Piece 1, 0–4 cm) (see “[Site 1158 Thin Sections](#),” p. 12), showing a plagioclase microphenocryst with concentric oscillatory zoning (top right) in a groundmass of plagioclase and clinopyroxene. The circular feature in the phenocryst is a glue bubble.



2 mm



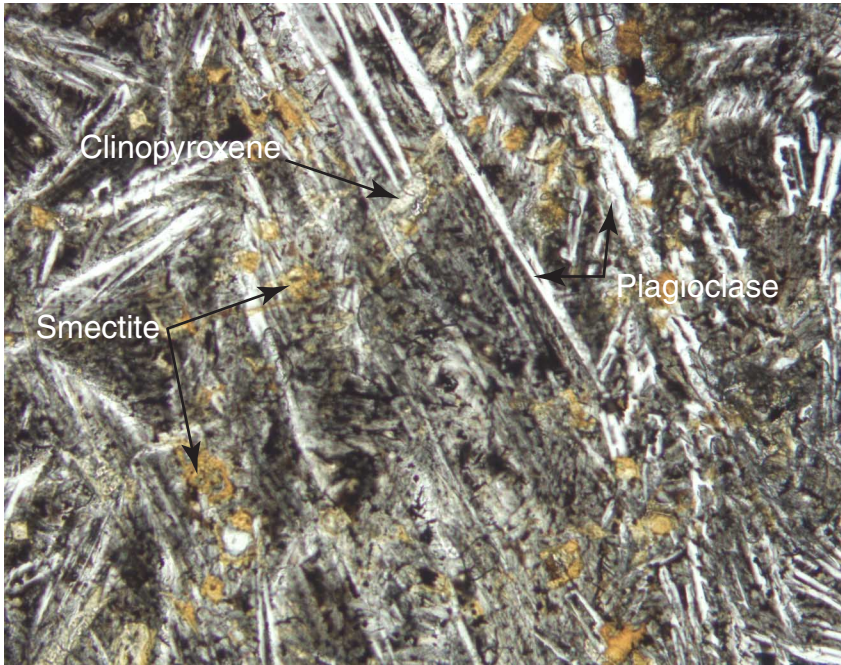
Figure F6. Photomicrograph, with crossed polars, of diabase Sample 187-1158C-2R-1 (Piece 13, 75–78) (see “Site 1158 Thin Sections,” p. 16), showing subophitic texture.



2 mm



Figure F7. Photomicrograph of basalt Sample 187-1158A-2R-1, 0–4 cm (see “Site 1158 Thin Sections,” p. 12), showing ~10% smectite replacement of groundmass.



1 mm



Figure F8. Photomicrograph of diabase Sample 187-1158C-2R-1, 75–78 cm (see “Site 1158 Thin Sections,” p. 16), showing Fe staining of plagioclase along cracks and cleavage planes, resulting from alteration of clinopyroxene.

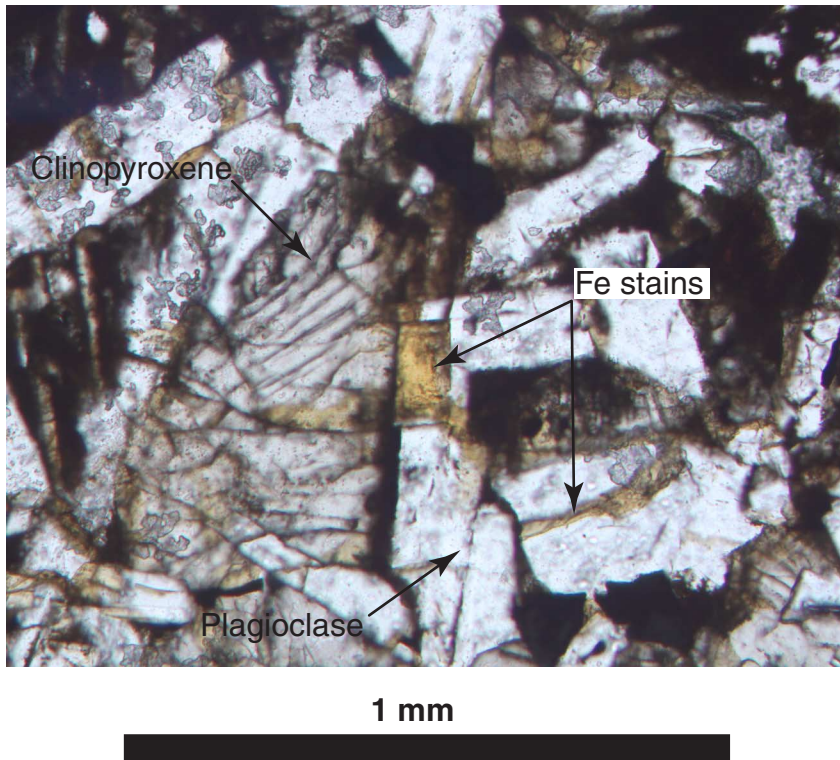


Figure F9. Seismic profile from *R/V Melville* cruise Sojourner 5 (00:00–01:59 Universal Time Coordinated, 26 February 1997) crossing the location of Site 1158. Shots are labeled every 15 min. Site 1158 is near shotpoint 680. Data have been filtered (1, 30, 375, 400), stacked, and migrated (90%).

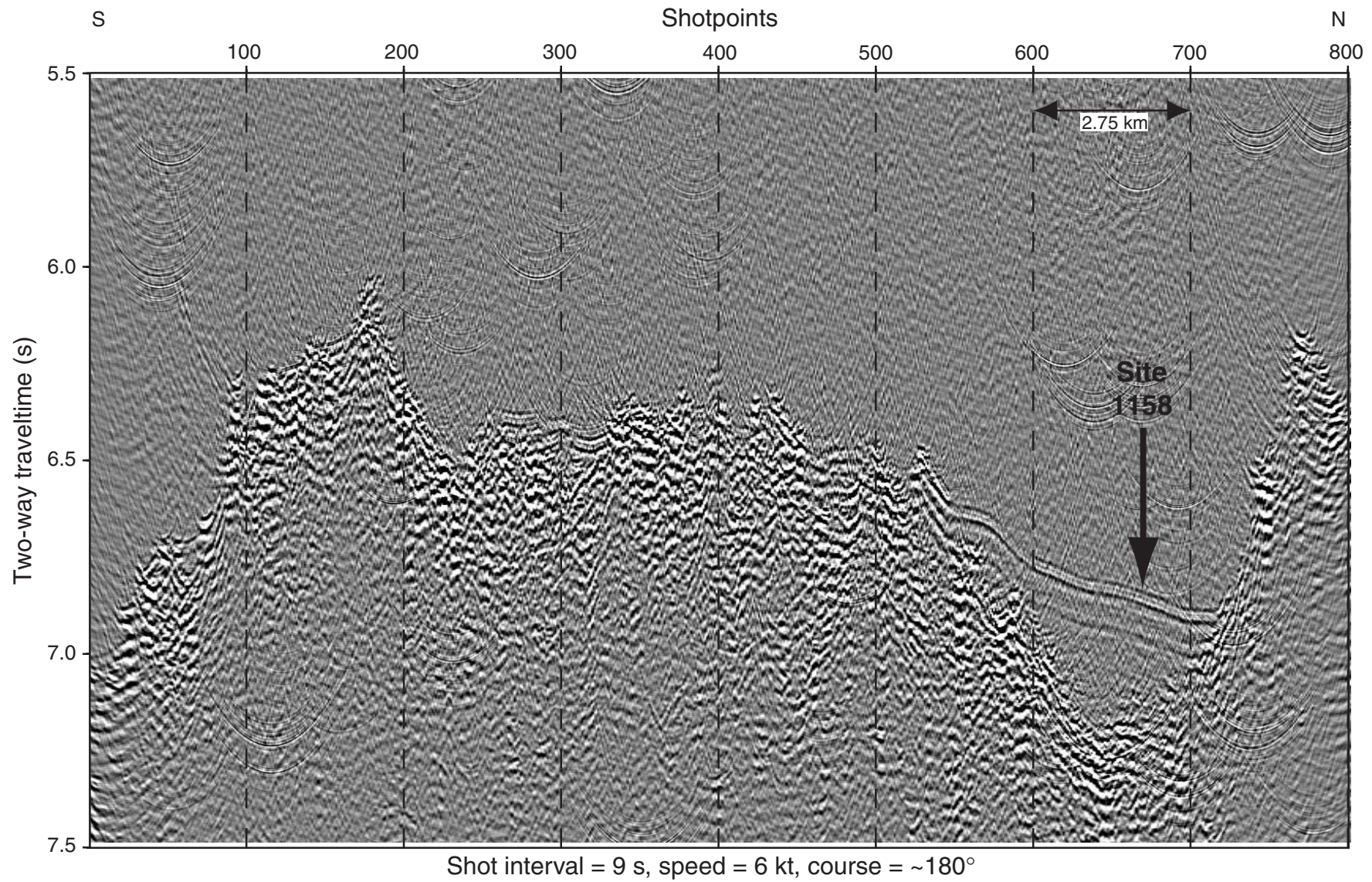


Figure F10. Major element compositions vs. MgO for Holes 1158A, 1158B, and 1158C basalt glass and whole-rock samples compared with Segments A2 and A3 zero-age basalt glasses. X-ray fluorescence (XRF) and ICP-AES data for splits of a single whole-rock powder are shown on all plots; therefore, two points represent each type of analysis for one sample. Only the average XRF or ICP-AES analyses reported in Table T3, p. 26, are plotted.

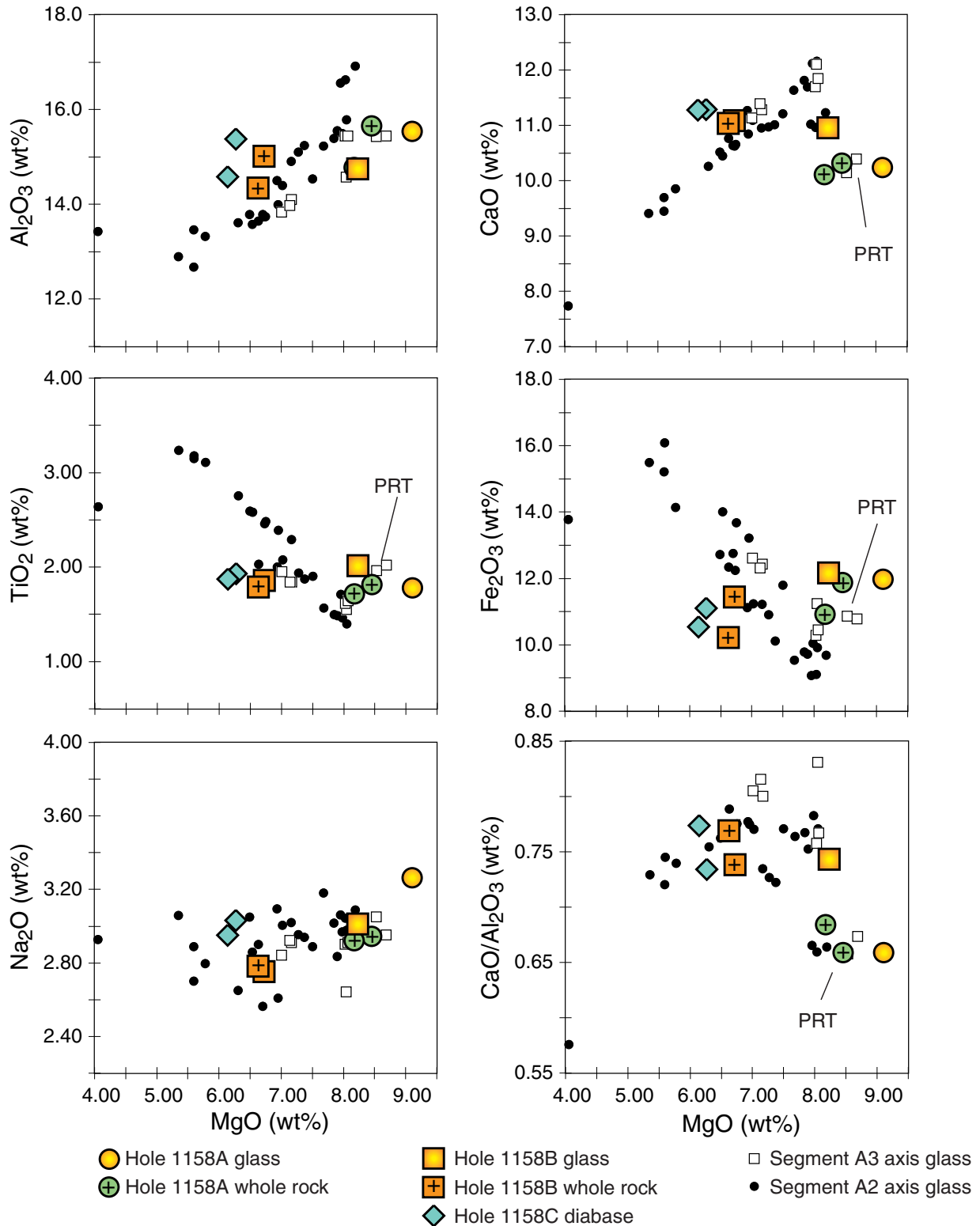


Figure F11. Trace element compositions vs. MgO for Holes 1158A, 1158B, and 1158C basalt glass and whole-rock samples compared with Segments A2 and A3 zero-age basalt glasses. X-ray fluorescence (XRF) and ICP-AES data for splits of a single whole-rock powder are shown on all plots; therefore, two points represent each type of analysis for one sample. Only the average XRF or ICP-AES analyses reported in Table T3, p. 26, are plotted. PRT = propagating rift tip lavas.

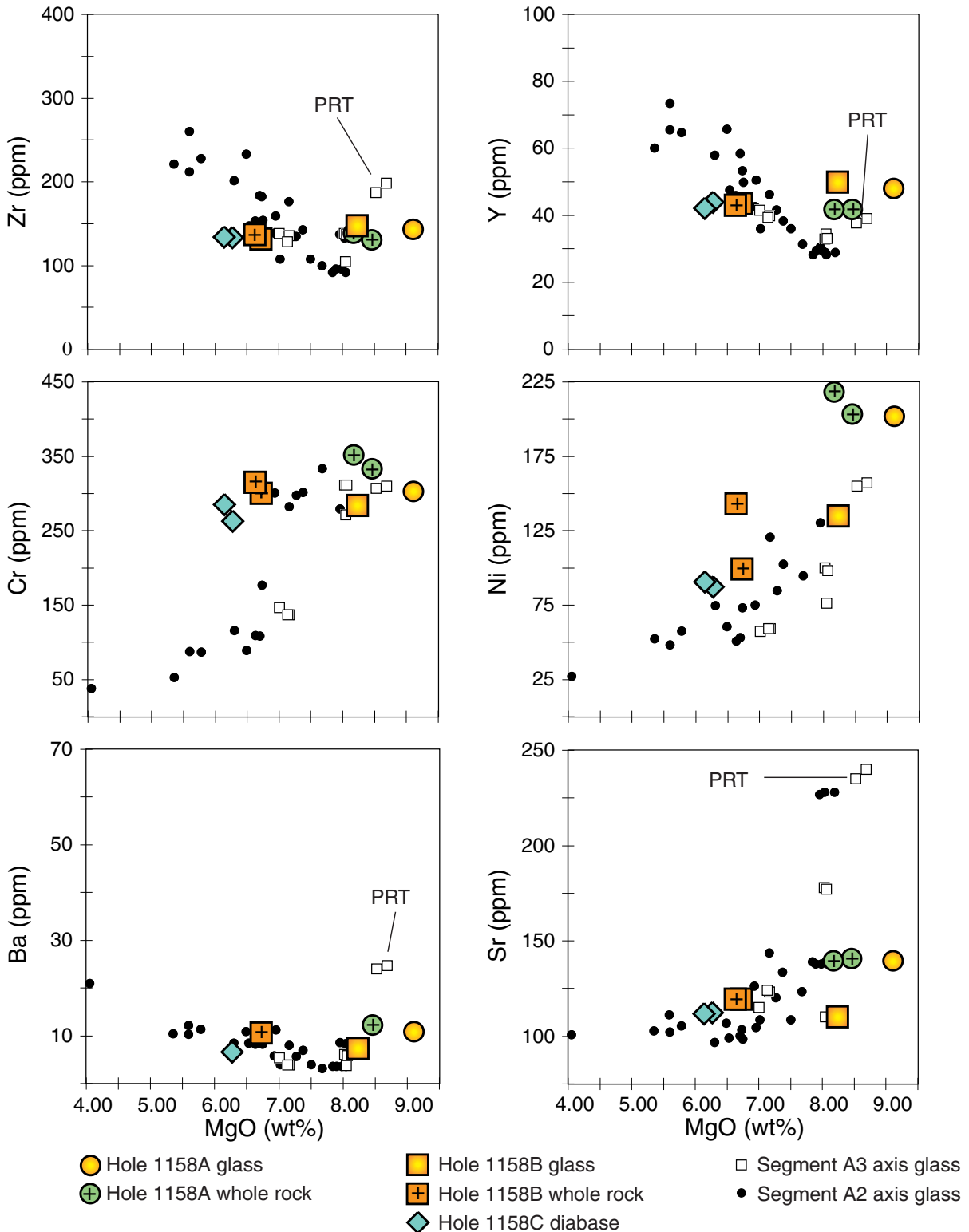


Figure F12. A. Variations of Zr/Ba vs. Ba of basaltic glass from Holes 1158A, 1158B, and 1158C and whole-rock samples compared with Indian- and Pacific-type mid-ocean-ridge basalt (MORB) fields defined by zero-age Southeast Indian Ridge (SEIR) lavas dredged between 123°E and 133°E. TP = Transitional Pacific; PRT = propagating rift tip lavas. B. Variations of Na₂O/TiO₂ vs. MgO for Holes 1158A, 1158B, and 1158C basaltic glass and whole-rock samples compared with Indian- and Pacific-type MORB fields defined by zero-age SEIR lavas dredged between 123°E and 133°E. A dashed line separates Indian- and Pacific-type zero-age SEIR basalt glass.

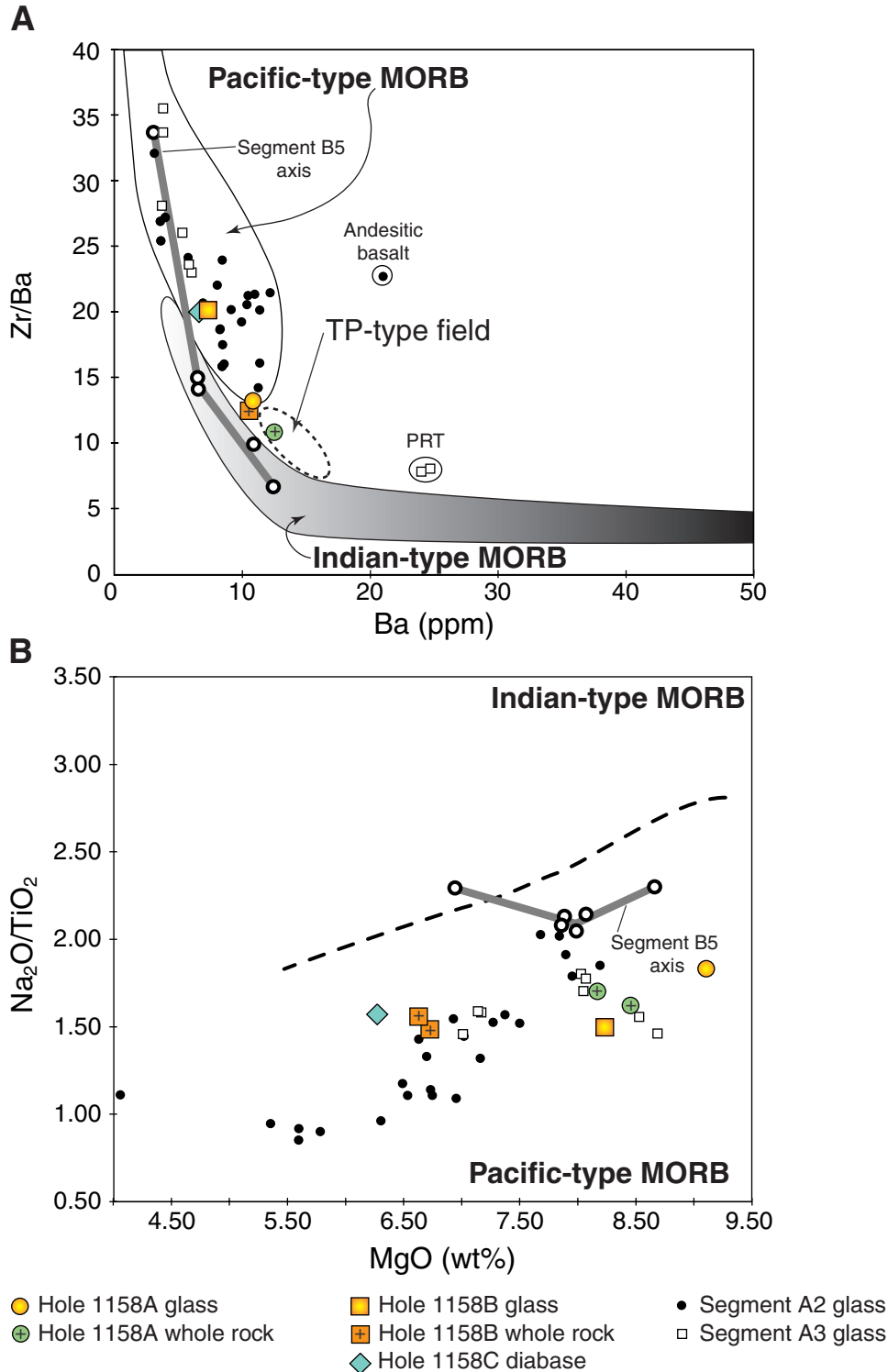


Table T1. Coring summary, Site 1158.

Hole 1158A

Latitude: 43°56.8970'S
 Longitude: 1128°49.6959'E
 Time on hole: 1715 hr, 15 Dec 99–1330 hr, 16 Dec 99 (20.25 hr)
 Time on site: 1715 hr, 15 Dec 99–2330 hr, 17 Dec 99 (54.25 hr)
 Seafloor (drill-pipe measurement from rig floor, mbrf): 5178.4
 Distance between rig floor and sea level (m): 11.1
 Water depth (drill-pipe measurement from sea level, m): 5167.3
 Total depth (from rig floor, mbrf): 5391.7
 Total penetration (mbsf): 213.3
 Total length of cored section (m): 14.4
 Total length of drilled intervals (m): 198.9
 Total core recovered (m): 0.85
 Core recovery (%): 5.9
 Total number of cores: 2
 Total number of drilled cores: 1

Hole 1158B

Latitude: 43°56.7837'S
 Longitude: 1128°49.7074'E
 Time on hole: 1330 hr, 16 Dec 99–0645 hr, 17 Dec 99 (16.25 hr)
 Seafloor (drill-pipe measurement from rig floor, mbrf): 5178.4
 Distance between rig floor and sea level (m): 11.1
 Water depth (drill-pipe measurement from sea level, m): 5167.3
 Total depth (from rig floor, mbrf): 5319.6
 Total penetration (mbsf): 141.2
 Total length of cored section (m): 15.0
 Total length of drilled intervals (m): 126.2
 Total core recovered (m): 1.6
 Core recovery (%): 10.7
 Total number of cores: 3
 Total number of drilled cores: 1

Hole 1158C

Latitude: 43°56.6782'S
 Longitude: 1128°49.7127'E
 Time on hole: 0545 hr, 17 Dec 99–2230 hr, 17 Dec 99 (17.75 hr)
 Seafloor (drill-pipe measurement from rig floor, mbrf): 5178.4
 Distance between rig floor and sea level (m): 11.1
 Water depth (drill-pipe measurement from sea level, m): 5167.3
 Total depth (from rig floor, mbrf): 5295.8
 Total penetration (mbsf): 117.4
 Total length of cored section (m): 9.4
 Total length of drilled intervals (m): 108.0
 Total core recovered (m): 1.61
 Core recovery (%): 17.1
 Total number of cores: 1
 Total number of drilled cores: 1

Core	Date (Dec 1999)	Ship local time	Depth (mbsf)		Length (m)		Recovery (%)	Comment
			Top	Bottom	Cored	Recovered		
187-1158A-								
1W	16	0815	0.0	198.9	198.9	1.91	N/A	
2R	16	1015	198.9	203.9	5.0	0.46	9.2	Whirl-Pak
3R	16	1215	203.9	213.3	9.4	0.39	4.1	
				Cored:	14.4	0.85	5.9	
				Drilled:	198.9			
				Total:	213.3			
187-1158B-								
1W	16	1900	0.0	126.2	126.2	1.56	N/A	
2R	16	2250	126.2	131.8	5.6	0.57	10.2	Whirl-Pak
3R	16	0210	131.8	136.8	5.0	0.18	3.6	
4R	16	0445	136.8	141.2	4.4	0.85	19.3	
				Cored:	15.0	1.60	10.7	
				Drilled:	126.2			
				Total:	141.2			
187-1158C-								
1W	17	1050	0.0	108.0	108.0	0.16	N/A	
2R	17	1315	108.0	117.4	9.4	1.61	17.1	Whirl-Pak
				Cored:	9.4	1.61	17.1	
				Drilled:	108.0			
				Total:	117.4			

Notes: N/A = not applicable. This table is also available in [ASCII](#) format.

Table T2. Rock samples incubated for enrichment cultures and prepared for DNA analysis and electron microscope studies and microspheres evaluated for contamination studies.

Core	Depth (mbsf)	Sample type	Enrichment cultures				DNA analysis			SEM/TEM samples	Microspheres [†]	
			Anaerobic	Aerobic	Microcosm*	High pressure	Wash	Centrifuged	Fixed	Air dried	Exterior	Interior
187-1158A-2R	198.9-203.9	Fine-grained basalt	9	3	1 Mn		X		X	X	Yes	Yes
187-1158C-2R	108.0-117.4	Fine-grained basalt Seawater	7	3	1 Fe/S	X	X		X	X	Yes	Yes
								X	X			

Notes: * = microcosm for iron and sulfur (Fe/S) or manganese (Mn) redox cycles; SEM = scanning electron microscope; TEM = transmission electron microscopy; † = contamination test; X = sample prepared on board. This table is also available in [ASCII](#) format.

Table T3. Glass and whole-rock major and trace element compositions of basalts, Site 1158.

Core, section:	Hole 1158A						Hole 1158B						Hole 1158C			
	3R-1	3R-1	3R-1	3R-1	3R-1	3R-1	2R-1	2R-1	2R-1	2R-1	4R-1	4R-1	2R-1	2R-1	2R-1	2R-1
Interval (cm):	0-3	0-3	10-13	10-13	10-13	10-13	55-58	55-58	55-58	55-58	34-38	34-38	75-78	75-78	75-78	75-78
Depth (mbsf):	203.9	203.9	204	204	204	204	126.75	126.75	126.75	126.75	137.14	137.14	108.75	108.75	108.75	108.75
Piece:	1	1	3	3	3	3	13	13	13	13	8	8	13	13	13	13
Unit:	1	1	1	1	1	1	1	1	1	1	1	1	2	2	2	2
Analysis:	ICP	ICP	ICP	ICP	XRF	XRF	ICP	ICP	XRF	XRF	ICP	ICP	ICP	ICP	XRF	XRF
Rock type:	Glass	Glass	Sparsely olivine-plagioclase phyric basalt				Sparsely olivine-plagioclase phyric basalt				Glass	Glass	Diabase	Diabase	Diabase	Diabase
Major element (wt%)																
SiO ₂	49.15	48.26	51.14	50.94	48.08	48.94	50.87	51.11	49.31	50.09	51.07	50.01	52.23	51.90	50.94	50.87
TiO ₂	1.79	1.77	1.84	1.79	1.70	1.73	1.87	1.84	1.75	1.82	2.01	2.01	1.91	1.95	1.87	1.88
Al ₂ O ₃	15.50	15.58	15.54	15.76	14.70	14.86	14.99	15.02	14.27	14.41	14.75	14.74	15.36	15.39	14.62	14.54
Fe ₂ O ₃	12.03	11.92	11.93	11.84	10.85	10.99	11.56	11.31	10.17	10.26	12.36	11.96	11.04	11.17	10.56	10.53
MnO	0.19	0.18	0.18	0.17	0.16	0.16	0.17	0.17	0.14	0.15	0.20	0.19	0.25	0.25	0.25	0.25
MgO	9.14	9.08	8.53	8.39	8.16	8.18	6.79	6.66	6.61	6.65	8.27	8.20	6.20	6.34	6.19	6.09
CaO	10.20	10.29	10.30	10.33	10.06	10.16	10.99	11.16	11.01	11.04	10.97	10.94	11.26	11.31	11.31	11.25
Na ₂ O	3.05	3.48	2.99	2.90	2.87	2.97	2.72	2.78	2.79	2.77	2.84	3.18	3.02	3.04	2.97	2.93
K ₂ O	0.13	0.13	0.42	0.43	0.36	0.37	0.42	0.43	0.33	0.34	0.10	0.11	0.21	0.22	0.20	0.20
P ₂ O ₅	0.19	0.21	0.20	0.19	0.17	0.18	0.19	0.19	0.17	0.18	0.21	0.22	0.19	0.19	0.18	0.18
LOI					0.41	0.41			1.24	1.24					0.35	0.35
CO ₂																
H ₂ O																
Total:	101.36	100.89	103.05	102.77	97.11	98.54	100.58	100.67	96.55	97.71	102.79	101.55	101.67	101.75	99.09	98.72
Trace element (ppm)																
Nb					5				4						5	
Zr	138	149	130	132	139		127	136	136		140	155	131	135	134	
Y	46	50	43	41	42		44	43	43		47	53	43	44	42	
Sr	139	141	140	141	140		118	121	119		109	111	111	114	112	
Rb					6				7						12	
Zn					92				96						98	
Cu					60				62						47	
Ni	199	204	204	203	218		100	98	143		134	135	88	87	91	
Cr	297	309	334	333	352		300	301	315		280	287	257	268	285	
V					271				309						335	
Ce					32				38						35	
Ba	11	11	12	12			11	11			7	7	7	7		
Sc	36	36	35	35			38	39			40	39	40	41		

Notes: LOI = loss on ignition. This table is also available in [ASCII](#) format.